2005

Exponential time response in analogue and Geiger mode avalanche photodiodes

C. Groves

C. H. Tan

J. P.R. David

G. J. Rees

Majeed M. Hayat

Exponential time response in analogue and Geiger mode avalanche photodiodes

C. Groves
Department of Electronic & Electrical Engineering, Sheffield University UK
C.H. Tan
Department of Electronic & Electrical Engineering, Sheffield University UK
J.P.R. David
Department of Electronic & Electrical Engineering, Sheffield University UK
G.J. Rees
Department of Electronic & Electrical Engineering, Sheffield University UK
M.M. Hayat
Department of Electrical and Computer Engineering at the University of New Mexico, Albuquerque, NM

Abstract

The mean avalanche current impulse response in an avalanche photodiode exhibits an initial transient and then grows or decays, above or below breakdown, at exponential rates which depend only on the probability distributions of the electron and hole ionization events. The process continues while the electric field profile remains unchanged by the applied bias or the evolving space charge. Below breakdown the distribution in the avalanche duration also exhibits an initial transient and then decays exponentially at the same rate as the mean current. Below breakdown the standard deviation in current decays exponentially at one half of the rate of the mean current, while above breakdown it grows exponentially at the same rate as the mean. Consequently the jitter in a Geiger mode avalanche photodiode becomes independent of time after the initial transients have decayed away. This behavior is quite general and independent of the electric field profile or of the presence of heterojunctions in the multiplication region. Using simple models for carrier transport we find the predicted enhancement in the velocity to ionization of those carriers which ionise shortly after their ballistic dead space significantly speeds up the avalanche dynamics in short devices.

SECTION I. Introduction

Impact ionization generates internal gain in an avalanche photodiode (APD). However, the multiple carrier transits of the avalanche region from ionization feedback processes delay the recovery of the diode, following optical excitation, to an extent which increases with the gain. Above breakdown the APD operates in the Geiger mode, so that a single absorbed photon can generate a measurable current. The avalanche build-up time is then also governed by these feedback processes, as is the standard deviation in the time taken to reach a predetermined threshold current chosen to register a breakdown event. This "jitter" increases the uncertainty in the time to breakdown and hence in the arrival time of the photon which may have triggered this event. These aspects of the time response of APDs are important features in determining the performance of the detection systems which they comprise.

Hayat and Saleh have shown analytically [1] that the mean avalanche current impulse response in an APD and its mean square value decay exponentially at long times, with an exponential rate given by the Malthusian parameter [2]. Their analysis assumed a multiplication region with a uniform electric field, that carriers travel always at constant speeds down the field and that the carrier ionization path length probability distribution functions (pdfs) are represented by exponentials, displaced to include the effects of dead space. We also observe this exponential decay at long times in our numerical modeling of APDs under more general conditions which relax the assumption of constant carrier velocities, and using a variety of techniques. These include Monte Carlo calculations of varying degrees of sophistication [3]–[4][5][6][7] and a recurrence equation technique [8] which allows for arbitrary carrier speeds to ionization and also for random fluctuations about these mean speEds., corresponding to diffusion.

Hayat and Dong [9] showed how to calculate the pdf of avalanche duration, the distribution in times for the last avalanche carrier to exit the multiplication region, under the same restrictive conditions as used in [1]. Ng et al. [10] generalized this technique by relaxing the conditions to those used in [8]. Both groups found that the pdfs of avalanche duration decay exponentially at long times.

Carrier diffusion appears to have only a small effect on the shapes of the current impulse response [3], [8] and of the avalanche duration pdf [10]. However, our modeling work [3]–[4][5][6], [11]–[12][13] predicts that those carriers which ionise at a distance shortly after the ballistic dead space, *d* travel to this early ionization event at an average speed which is considerably higher than for carriers which ionise further downstream. We expect the effect to be important in thin APDs and that it more than compensates [5] for the slowing effect of dead space

[1] which increases the number of carrier excursions back and forth across the multiplication region to maintain gain [7].

We have shown [14] that this speed enhancement can be explained in terms of the reduction in scattering which causes carriers to ionise at short distances. We have also argued [14], using simple models, that the mean speed, $v(z)$ to ionization at a distance z after the carrier is injected cold can be written approximately as $v(z)=v0(1-d/z)-1$, where $v0$ is the limiting value of $v(z)$ at long ionization path lengths. Indeed, this simple expression describes very well the behavior which we observe in our numerical simulations.

In this note we generalize the technique of Hayat and Saleh [1], relaxing some of their restrictive assumptions, to show how both the mean and the mean squared avalanche current impulse response in an APD depend exponentially on time, following the initial transients, and how these exponential rates are related to the probability distributions of the ionization events. The arguments apply both below breakdown and also above it, when the device operates in Geiger mode, resulting respectively in exponential decay and growth, provided the effects of space charge and of external quenching processes can be ignored. The behavior of the standard deviation in the current is examined below and above breakdown, as is the behavior of jitter, which is predicted to become independent of time in Geiger mode operation. We also show that, following the initial transients, the pdf of avalanche duration decays at the same exponential rate as the mean avalanche current.

We demonstrate that this behavior is to be expected, irrespective of the electric field profile in the multiplication layer, thus allowing for the effects of residual, unintentional doping, of depletion into the p- and n-contacts and for the presence of heterojunctions. We assume the most general form for ionization event pdfs and require only that the arbitrary field profile remain constant during the avalanche process. The results therefore hold only while the avalanche space charge remains small, since this will have a significant effect on the field profile at macroscopic current levels, and before external quenching reduces the applied bias. These exponential rates are then evaluated numerically for specific cases, assuming constant carrier velocities and also allowing for the predicted enhancement in velocity to early ionization. It should be noted that the model presented is one dimensional and therefore does not consider jitter associated with lateral diffusion of carriers to the edge of the breakdown region.

SECTION II. Mean Current Response

When the ionising electric field depends upon position in the multiplication region then the ionization event pdfs depend on the time, τ elapsed between carrier injection and ionization and also on its position, z of injection, as well as its position, z' of ionization [15], and not only on their difference, $z'-z$. The ionization event pdf for electrons (holes) then takes the form $he(h)(z,z',\tau)$ instead of the simpler, conventionally assumed form, $he(h)(|z'-z|,\tau)$ appropriate for a uniform field.

Tan et al. [8] derive equations [their (1) and (2)] for the mean current impulse response at time t, $\langle Ie(h)(z,t)\rangle$, resulting from injection of an electron (hole) at position z and time $t=0$ into a multiplication region with uniform electric field and width w. We can generalize their equations to nonuniform field to find

(1a) top

(1b) bottom

$$\langle I_e(z,t)\rangle = \quad P_e(z,t)\langle I_{e0}(z,t)\rangle + \int_z^w dz' \int_0^t d\tau h_e(z,z',\tau) \cdot (2\langle I_e(z',t-\tau)\rangle + \langle I_h(z',t-\tau)\rangle)$$

$$\langle I_h(z,t)\rangle = \quad P_h(z,t)\langle I_{h0}(z,t)\rangle + \int_0^z dz' \int_0^t d\tau h_h(z,z',\tau) \cdot (2\langle I_h(z',t-\tau)\rangle + \langle I_e(z',t-\tau)\rangle).$$

Here electrons are imagined to drift from left to right and holes from right to left. The first terms on the right-hand side of these equations represent the contributions from the injected, primary currents, ⟨*Ie*(*h*)0(*z*,*t*)⟩, and

(2a) top

(2b) bottom

$$P_e(z,t) \quad = 1 - \int_z^w dz' \int_0^t d\tau h_e(z,z',\tau)$$

$$P_h(z,t) \quad = 1 - \int_0^z dz' \int_0^t d\tau h_h(z,z',\tau)$$

are the probabilities that the injected carriers avoid ionising before exiting the multiplication region before time *t*.

After these primary current contributions have died away we can, following Hayat and Saleh [1], seek asymptotic, exponentially decaying solutions for the remaining currents, $\langle I_{e,h}(z,t)\rangle = i_{e,h}(z)\exp(-\gamma t)$, which result only from carriers generated by impact ionization. Substituting this form in (1), in the absence of the primary current terms we find

(5a) and (5b)

$$i_{2e}(z) = \int_z^w dz' \int_0^t d\tau h_e(z,z',\tau)\exp(\delta\tau)\left(\begin{matrix}2i_{2e}(z') + i_{2h}(z') \\ +\{2i_e^2(z') + 4i_h(z')i_e(z')\}\exp\{-(2\gamma-\delta)(t-\tau)\}\end{matrix}\right)$$

$$i_{2h}(z) = \int_0^z dz' \int_0^t d\tau h_h(z,z',\tau)\exp(\delta\tau)\left(\begin{matrix}2i_{2h}(z') + i_{2e}(z') \\ +\{2i_h^2(z') + 4i_e(z')i_h(z')\}\exp\{-(2\gamma-\delta)(t-\tau)\}\end{matrix}\right)$$

(3a) and (3b)

$$i_e(z) = \int_z^w dz' g_e(z,z';\gamma)\{2i_e(z') + i_h(z')\}$$

$$i_h(z) = \int_0^z dz' g_h(z,z';\gamma)\{2i_h(z') + i_e(z')\}$$

Where

(4a)

$$g_{e,h}(z,z';\gamma) \equiv \int_0^\infty h_{e,h}(z,z',\tau)\exp(\gamma\tau)d\tau\,.$$

View Source Here we have used the fact that, since the ranges of z and z' are limited, $he,h(z,z',\tau)$ vanishes for large τ and we can replace the upper limit, t in the integral by ∞.

The consistency of the coupled, homogeneous, linear (3) constitutes a condition which determines the value of γ, the Malthusian parameter [2] which depends only on the form of the $he,h(z,z',\tau)$. When this condition is satisfied the solutions, $ie,h(z)$ are also determined to within an arbitrary, multiplicative constant.

SECTION III. Mean Squared Current Response

Tan et al. [8] also derive equations [their (3) and (4)] for the mean squared current impulse response, $\langle I2e(h)(z,t)\rangle$ at time t. Again, generalizing to nonuniform field and after the primary currents have died away, we can extract the asymptotic exponential behavior by writing $\langle I2e(h)(z,t)\rangle \sim i2e(h)(z)\exp(-\delta t)$, to find (5), shown at the bottom of the page. Here the $ie(h)(z)$ are as defined earlier and given by (3).

For an APD biased below breakdown $\gamma>0$. If we suppose that $2\gamma-\delta>0$ then the terms involving $\exp\{-(2\gamma-\delta)(t-\tau)\}$ are asymptotically small and (5) can be cast in the form of (3), with $i2e(h)(z)$ replacing $ie(h)(z)$. It follows that $\delta=\gamma$, confirming our supposition that $2\gamma-\delta>0$ and consistent with [1].

The standard deviation in the currents, given by

(6)

$$\sigma_{e(h)}(z,t) \sim \sqrt{i_{2e(h)}(z)\exp(-\delta t) - (i_{e(h)}(z))^2\exp(-2\gamma t)}$$

with $\delta=\gamma$, behaves asymptotically as $\sim\exp(-\gamma t/2)$, since the second term under the square root decays faster than the first.

In the case of an APD biased above breakdown to operate in Geiger mode then $\gamma<0$ and the mean asymptotic impulse response current grows exponentially. If we again suppose that $2\gamma-\delta>0$, then again we find $\delta=\gamma$, for the same reasons as before. However, this time it follows that $2\gamma-\delta=\gamma$ is negative, contrary to our supposition, which

therefore cannot be correct. If, on the other hand, we suppose that $2\gamma-\delta<0$, then the terms involving $\exp\{-(2\gamma-\delta)(t-\tau)\}$ diverge at long times and dominate the right-hand side of (5), which increase as $\exp(-2\gamma t)$, in contrast to the left-hand sides, which are independent of time, also ruling out this supposition. There remains only the possibility that $\delta=2\gamma$, when (5) become inhomogeneous integral equations for $i2e(z)$ and $i2h(z)$. Thus, for an APD biased above breakdown with $\gamma<0$, we find that $\delta=2\gamma$, so that the standard deviation in the current in (6) in this case behaves asymptotically as $\sigma e(h)(z,t)\sim\exp(-\gamma t)$.

We arrive at the curious result that below breakdown $\sigma\sim\exp(-\gamma t/2)$, whereas above breakdown $\sigma\sim\exp(-\gamma t)$, where γ is the Malthusian parameter [2] describing the decay or growth of the mean current. Interestingly, this type of asymmetrical asymptotic behavior in the second moment, above and below breakdown, is also seen in other models of population dynamics (see [2]).

SECTION IV. Avalanche Duration

Ng et al. [10] derive equations for the probability, $Fe(h)(z,t)$ that, below breakdown, an avalanche, initiated by injecting an electron (hole) at position z in a uniform multiplication region at time $t=0$, terminates before time t [their (2) and (3)]. Again we can generalize these equations to the case of nonuniform fields, so that

(7a) top

(7b) bottom

$$F_e(z,t) = P_e(z,t)Q_e(z,t) + \int_z^w dz' \int_0^t d\tau h_e(z,z',\tau) \cdot F_e^2(z',t-\tau)F_h(z',t-\tau)$$

$$F_h(z,t) = P_h(z,t)Q_h(z,t) + \int_0^z dz' \int_0^t d\tau h_h(z,z',\tau) \cdot F_h^2(z',t-\tau)F_e(z',t-\tau).$$

Here $Qe(h)(z,t)$ represents the probability that an electron (hole) injected at position z escapes the multiplication region before time t has elapsed. In fact the original (2) and (3) in [10] are in error and the Pe,h depend also on t, as well as on z, as correctly acknowledged here in our (2).

The pdfs of avalanche duration following electron (hole) injection are given by $fe(h)(z,t)=\partial Fe(h)(z,t)/\partial t$ and can be evaluated by differentiating (7). After waiting sufficiently long (of the order of a carrier transit time) for the inhomogeneous terms on the right of these equations to die away we find, for the electron initiated avalanche duration pdf,

(8)

$$f_e(z,t) = \int_z^w dz' h_e(z,z',t) F_e^2(z',0) F_h(z',0) + \int_z^w dz' \int_0^t d\tau h_e(z,z',\tau) \times \begin{pmatrix} 2f_e(z',t-\tau)F_e(z',t-\tau)F_h(z',t-\tau) \\ +f_h(z',t-\tau)F_e^2(z',t-\tau) \end{pmatrix}.$$

At time *t*=0 the probabilities *Fe*(*h*)(*z*,*t*) are zero so that the first term on the right-hand side of (8) is also zero. At long times these probabilities approach unity so that the equation then simplifies to

(9a)

$$f_e(z,t) = \int_z^w dz' \int_0^t d\tau h_e(z,z',\tau) \cdot \{2f_e(z',t-\tau) + f_h(z',t-\tau)\}.$$

View Source Similar arguments for hole injection yield

(9b)

$$f_h(z,t) = \int_0^z dz' \int_0^t d\tau h_h(z,z',\tau) \cdot \{2f_h(z',t-\tau) + f_e(z',t-\tau)\}.$$

These equations are identical in form to (1), after the primary currents have decayed away, with ⟨*Ie*,*h*(*z*,*t*)⟩ replaced by *fe*,*h*(*z*,*t*). It follows that the avalanche duration pdfs decay exponentially in time at the same exponential rate as the mean avalanche current.

When the multiplication region is uniform then the *he*(*h*)(*z*,*z*′,*τ*) depend only on the difference *z*−*z*′ and not separately on *z* and *z*′, so that we can write *he*(*z*,*z*′,*τ*)=*he*(*z*′−*z*,*τ*) and *hh*(*z*,*z*′,*τ*)=*hh*(*z*−*z*′,*τ*). It follows from (3a) and (3b) that

(3c) top

(3d) bottom

$$i_e(z) = \int_z^w dz' g_e(z'-z;\gamma)\{2i_e(z') + i_h(z')\}$$

$$i_h(z) = \int_0^z dz' g_h(z-z';\gamma)\{2i_h(z') + i_e(z')\}$$

where

(4b)

$$g_{e,h}(\zeta\gamma) \equiv \int_0^\infty h_{e,h}(\zeta,\tau)\exp(\gamma\tau)\,d\tau.$$

In the general case we could attempt to find *γ* by discretizing the integrals in (3) to generate a set of linear equations from which we could find numerically the value of *γ* which gave nontrivial solutions for *ie*,*h*(*x*). However, as shown by Hayat and Saleh [1], for simple forms of *he*(*h*)(*ζ*,*τ*) we can make further analytical progress.

SECTION V. Models for *he*,*h*

A. Dead Space and Constant Carrier Velocity

Hayat and Saleh [1] used a displaced exponential model for the spatial part of h_e and assumed that electrons travel always at their constant speeds v_e so that

$$\begin{aligned} h_e(\zeta,\tau) &= 0, \text{for} \zeta < d_e \\ h_e(\zeta,\tau) &= \alpha\exp\{-\alpha(\zeta-d_e)\}\delta(\tau-\zeta/v_e), \text{for} \zeta > d_e \end{aligned}$$

where *de* represents the electron dead space. It follows that

(10a) and (10b)

$$\begin{aligned} g_e(\zeta;\gamma) &= 0, \text{for} \zeta < d_e \\ g_e(\zeta;\gamma) &= \alpha\exp\{-\alpha(\zeta-d_e)+\gamma\zeta/v_e\}, \text{for} \zeta > d_e. \end{aligned}$$

B. Dead Space and Enhanced Carrier Velocity

Assuming a conventional displaced exponential for the spatial part of *he* but that the electron velocity to ionization at position *ζ* downstream from the injection point is given by $v_e(\zeta) = v_e(1-d_e/\zeta)^{-1}$, then we find

$$\begin{aligned} h_e(\zeta,\tau) &= 0, \text{for} \zeta < d_e \\ h_e(\zeta,\tau) &= \alpha\exp\{-\alpha(\zeta-d_e)\}\delta(\tau-(\zeta-d_e)/v_e)\zeta > d_e \end{aligned}$$

So that

(11a) and (11b)

$$\begin{aligned} g_e(\zeta;\gamma) &= 0, \text{for} \zeta < d_e \\ g_e(\zeta;\gamma) &= \alpha\exp\{-(\alpha-\gamma/v_e)(\zeta-d_e)\}, \text{for} \zeta > d_e. \end{aligned}$$

We can summarize the results of both of these models by defining $\alpha*=\alpha-\gamma/v_e$. Then

(12a) and (12b)

$$\begin{aligned} g_e(\zeta;\gamma) &= 0, \text{for} \zeta < d_e \\ g_e(\zeta;\gamma) &= \alpha\exp(-\alpha*\zeta), \text{for} \zeta > d_e \end{aligned}$$

where for the constant velocity model $a=\alpha\exp(\alpha d_e)$ and for the enhanced velocity model $a=\alpha\exp(\alpha * de)$.

When $de=0$ both of these models collapse into the conventional, local, constant velocity model, giving

(13)

$$g_e(\zeta;\gamma) = \alpha \exp\left\{\zeta\left(\frac{\gamma}{v_e} - \alpha\right)\right\}.$$

The corresponding expressions for holes throughout are found by replacing $g_e(\zeta;\gamma), \alpha, \alpha *, a, v_e$, and de and with $g_h(\zeta;\gamma), \beta, \beta *, b, v_h$.

SECTION VI. Solution for γ

Substituting (12) and the corresponding expressions for holes into (3) we find

(14a) and (14b)

$$i_e(z) = \int_{z+d_e}^{w} a\exp\{\alpha * (z-x)\}\{2i_e(x) + i_h(x)\}dx$$
$$i_h(z) = \int_{0}^{z-d_h} b\exp\{\beta * (x-z)\}\{2i_h(x) + i_e(x)\}dx\,.$$

Multiplying these equations respectively by $\exp(-\alpha * z)$ and $\exp(\beta * z)$ and differentiating with respect to z we find

(15a) and (16b)

$$i_e'(z) - \alpha * i_e(z) = -a\exp(-\alpha * d_e)\{2i_e(z+d_e) + i_h(z+d_e)\}$$

$$i_h'(z) + \beta * i_h(z) = b\exp(-\beta * d_h)\{2i_h(z-d_h) + i_e(z-d_h)\}.$$

The boundary conditions on ie,h are found from the integral equations (14)

(16a) and (16b)

$$i_e(w-d_e) = 0$$
$$i_h(d_h) = 0.$$

Equations (15) admit solutions of the form

(17a) and (17b)

$$i_e(z) = E\exp(mz)$$
$$i_h(z) = H\exp(mz)$$

where the equation for m

(18)

$$\{(\alpha * -m)\exp\{(\alpha * -m)d_e\} - 2a\}$$
$$\{(\beta * +m)\exp\{(\beta * +m)d_h\} - 2b\} - ab = 0$$

is found by substituting (17) into (15) and eliminating E and H. Where the roots of (18) are complex these occur in conjugate pairs since (18) is a real equation for *m*.

(22)

$$((\alpha * -m\_1)\exp\{\alpha * d\_e + m\_1\,(d\_h - w)\} - 2a\exp\{m\_1\,(d\_h + d\_e - w)\} - (\alpha * -m\_2)\exp\{\alpha * d\_e + m\_2\,(d\_h - w)\} + 2a\exp\{m\_2\,(d\_h + d\_e - w)\} = 0.$$

When *de*,*h*=0 (18) turns into a quadratic equation for *m* with two roots, *m*=*m*1,2. We find (18) also has two roots when *de*,*h*≠0, though we must find these solutions, *m*1,2 numerically.

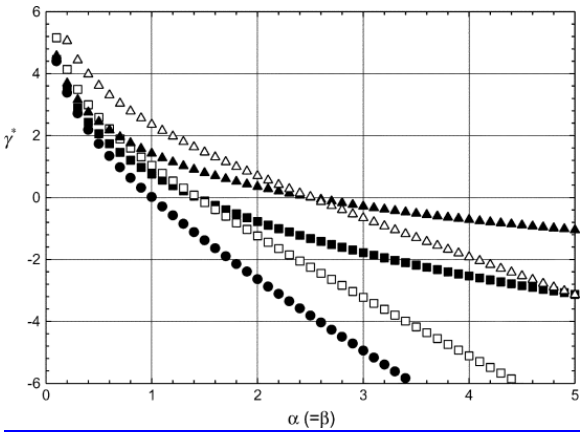

Fig. 1. *γ*∗ versus *αw* for *de*/*w*=0 (circles), 0.1 (squares), and 0.2 (triangles), for the constant (filled) and enhanced velocity (open) models. *ve*=*vh*,*de*=*dh*, and *α*=*β* in all cases. The constant and enhanced velocity models coincide at *de*=0=*dh*, as do their results.

We can then seek general solutions for (15) of the form

(19a) and (19b)

$$i_e(z) = A\exp(m_1 z) + C\exp(m_2 z)$$
$$i_h(z) = B\exp(m_1 z) + D\exp(m_2 z).$$

Substituting these solutions into (15a) and equating the coefficients of the terms in exp(*m*1*z*) and in exp(*m*2*z*) we find

(20a) and (20b)

$$\frac{B}{A} = \frac{[(\alpha * -m_1)\exp\{(\alpha * -m_1)d_e\} - 2a]}{a}$$
$$\frac{D}{C} = \frac{[(\alpha * -m_2)\exp\{(\alpha * -m_2)d_e\} - 2a]}{a}.$$

Applying the boundary conditions (16) to the solutions (19) gives

(21a) and (21b)

$$\frac{A}{C} = -\exp\{(m_2 - m_1)(w - d_e)\}$$
$$\frac{B}{D} = -\exp\{(m_2 - m_1)d_h\}.$$

Finally we combine (20) and (21), eliminating A, B, C, and D, to find (22), shown at the bottom of the page. Equation (22) constitutes an equation for *γ*, whose solution can be found numerically.

An alternative and equivalent condition on *γ* may also be found by substituting (19) into (15b) and again using (21) to eliminate the coefficients. When the roots *m*1 and *m*2 of (18) are complex conjugates the real part of the left-hand side of (22) is identically zero and *γ* is found from the zero of the imaginary part.

SECTION VII. Results

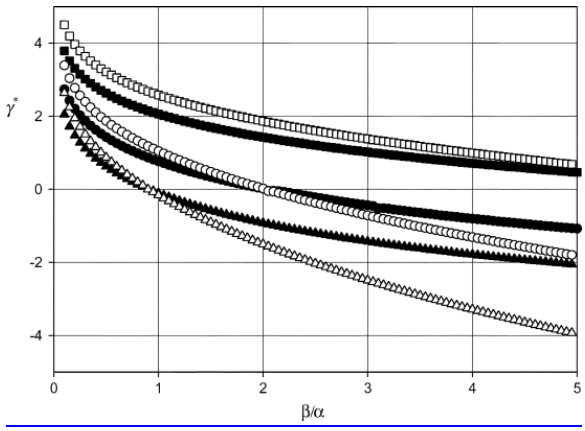

Fig. 2. *γ*∗ versus *β*/*α* for *αw*=0.5 (squares), 1.0 (circles), and 1.5 (triangles), for the constant (filled) and enhanced velocity (open) models. v_e=v_h and $d_e w$=0.1=$d_h w$ in all cases.

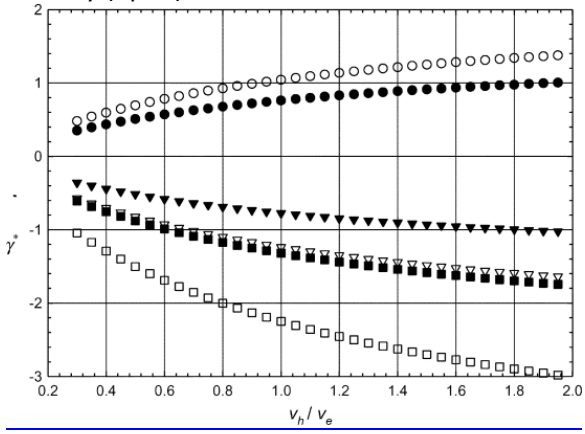

Fig. 3. *γ*∗ versus v_h/v_e for (circles) *αw*=0.5, (triangles) 1.0, and (squares)2.0, for the constant (filled) and enhanced velocity (open) models. *β*=*α* and *dew*=0.1=$d_h w$ in all cases.

Equation (22) was solved numerically to find the Malthusian parameter *γ* for a range of values of multiplication region width *w*, enabled ionization coefficients *α* and *β* for electrons and holes, velocities to ionization *ve* and *vh*, and dead spaces *de* and *dh*. Results were derived using both the models for constant [(10)] and enhanced [(11)]

velocities to ionization and are plotted in terms of the dimensionless quantity $\gamma^* \equiv \gamma w / v_e$, the Malthusian parameter normalized to the electron "transit" time, w/v_e.

Fig. 1 shows γ^* as a function of the dimensionless electron ionization coefficient, αw, plotted for a range of values of d_e/w and assuming equal ionization parameters for electrons and holes. When d_e/w=0 the constant and enhanced velocity models coincide, as do the corresponding results. For smaller values of αw, corresponding to weaker ionization, γ^* is positive so that the current impulse response to injected carriers ultimately decays with time, as in an APD. As αw is increased γ^* falls, changing sign when the device breaks down (corresponding to αw=1 when the dead space is zero) so that the current impulse response ultimately grows exponentially with time, as in a SPAD. The value of αw at breakdown increases with d_e/w, as might be expected since, as dead space is increased, a greater portion of the avalanche region is denied to multiplication and the ionization coefficients must increase to compensate. For any values of αw and d_e/w the absolute value of γ^* is always larger for the enhanced velocity model than for the constant velocity model of ionization, confirming that the velocity enhancement accelerates both the decay in the current response in an APD operated below breakdown and its growth in an APD operated in Geiger mode. The breakdown value of αw (where γ^*=0) is the same for both models, as might be expected since multiplication depends only on the number of ionization events and not on the speed with which they happen.

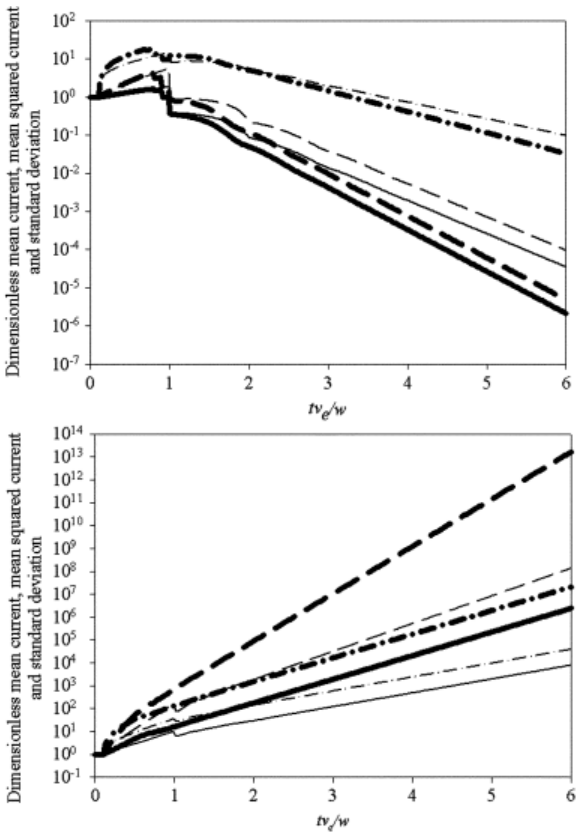

Fig. 4. (Full lines) Dimensionless mean current, (dashed lines) mean squared current and (dash-dot lines) current standard deviation, assuming constant (faint) and enhanced (bold) velocities to ionization versus dimensionless time, tv_e/w, assuming equal ionization parameters for electrons and holes, with d_e/w=0.1. (a) Below breakdown, with αw=0.5 and (b) above breakdown, with αw=2.5.

Fig. 2 shows curves of γ^* against β/α, assuming equal values for other electron and hole ionization parameters, at a value of d_e/w=0.1 and for a range of values of αw. For any value of αw the current decays for small values of β/α but increasing this ratio pushes the device through breakdown, as does increasing αw.

Fig. 3 shows the effect on $\gamma*$ of the hole/electron velocity ratio, v_h/v_e with other electron and hole ionization parameters equal, for d_e/w=0.1 and for a range of values of αw. As v_h decreases, so that v_h/v_e falls toward zero for fixed v_e, so the dynamical behavior, asymptotic decay below breakdown or growth above, depending on the value of αw, becomes slower. The asymptotic behavior described here depends on the cooperation of both electrons and holes and when one set of carriers becomes fixed the process stops. As v_h/v_e becomes large the rates saturate since they are then limited only by the speed of the electrons.

Fig. 4 shows the mean impulse current response to pure electron injection, normalized to the injected primary current, qve/w, the mean of the square of this quantity and the normalized current standard deviation, calculated by solving numerically the recurrence equations derived in [8]. We assume equal ionization parameters for electrons and holes, take de/w=0.1,ve=105 m/s and w=1 μm and calculate the responses for αw=0.5 (below breakdown) in Fig. 4(a) and αw=2.5 (above breakdown) in

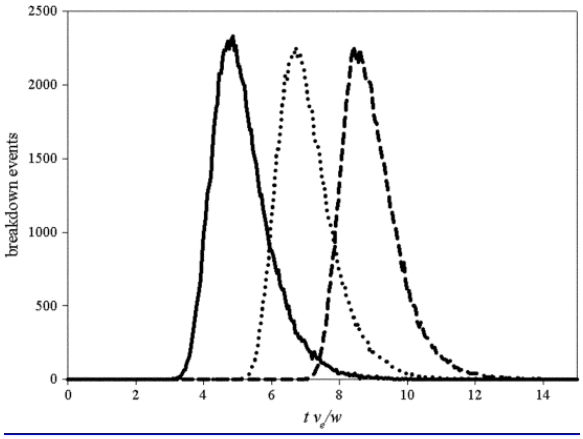

Fig. 5. RPL calculations of distributions of times to reach avalanche currents of (full line) 0.01 mA, (dotted line) 0.1 mA, and (dashed line) 1 mA assuming de/w=0.1 with αw=2.5 and identical ionization parameters for electrons and holes.

Fig. 4(b). Both above and below breakdown the curves show transient behavior at early times and then settle down to exponential growth and decay respectively. Including velocity enhancement in the model for the ionization process clearly speeds up the dynamical behavior at long times and detailed inspection shows that the exponential rate constants are as predicted by (22). These numerical solutions also confirm the analytical predictions that the mean current and the mean squared current exhibit the same exponential decay rate, γ below breakdown, so that the standard deviation in the current decays as $\gamma/2$. By contrast, above breakdown the mean squared current grows with an exponential rate twice that of the mean current, so that the standard deviation in current grows with the same exponential growth rate as its mean, also as predicted analytically.

The jitter, defined here as the standard deviation in time before reaching a predetermined threshold current chosen to register a breakdown event, limits the precision with which this event, and hence the arrival of any photon which stimulated it, can be located in time. This jitter can be estimated by dividing the standard deviation in current, $\sigma_{e(h)}(z,t)$ by the slope of the mean current response, $\partial\langle I_{e(h)}(z,t)\rangle/\partial t$. Since these two quantities increase exponentially at the same rate we expect the jitter in a Geiger mode APD to be independent of time at long times. It follows that the jitter first undergoes a transient behavior, following initiation of the breakdown event, and then becomes independent of current when this is growing exponentially.

This analytical prediction is supported by the numerical calculations in Fig. 4(b) of the mean impulse response current and its standard deviation. It is also supported by independent random path length (RPL) calculations [13] of the distributions of times taken to reach threshold currents spanning two decades, an example of which

is shown in Fig. 5. In this example a Monte Carlo scheme is used to select the random positions and times of the ionization events in an avalanche process according to the displaced exponential, constant velocity ionization event pdfs leading to (10). This independence of jitter on time in a device operated above breakdown has also been observed in earlier Monte Carlo simulations [16]. Below breakdown the jitter is predicted to grow exponentially, at a rate $\gamma/2$.

SECTION VIII. Summary and Discussion

A technique was derived to calculate the rates of exponential growth or decay of the mean impulse response current and its standard deviation in an APD biased above or below breakdown, together with the pdfs of avalanche duration below breakdown. The exponential rate γ is found by requiring the consistency of homogeneous integral equations whose kernels are the Laplace transforms of the pdfs of ionization events for the ionising carriers. The exponential behavior described here is quite general and is independent of the electrical field profile of the multiplication region and of the presence of heterojunctions, provided the field profile remains independent of time. Moreover the (3) from which γ is calculated are independent of the initial injection conditions, as is the asymptotic behavior which γ describes.

These rate constants are evaluated ignoring the effects of carrier diffusion and the results are compared for the cases when carrier velocities to ionization are assumed constant, and also allowing for the velocity enhancement to ionization associated with the reduced scattering predicted for carriers which ionise shortly after their ballistic dead space. For short multiplication regions designed for high speed the velocity enhancement leads to significantly faster dynamical behavior, both above and below breakdown.

The exponential time behavior discussed here strictly applies asymptotically. However, it is apparent from Fig. 4 that it appears to become well established after an initial transient which lasts a few carrier transit times of the multiplication region and corresponds to a decade or so of current increase. In an APD biased below breakdown exponential current decay can be expected to continue until chance fluctuations stop the current and the multiplication process terminates, although, strictly speaking we are here concerned with the mean current, averaged over many trials, which continues to decay indefinitely.

In a Geiger mode device other factors intervene to limit the exponential growth in mean current above breakdown. Conventionally the avalanche current is quenched with a series ballast resistor, or active quenching circuit, chosen so that the saturated avalanche current does not exceed $\sim$20 μA [17] so that a statistical fluctuation is then likely to terminate the avalanche process. The primary current due to the injected carrier is given by Ramo's theorem as qv/w, where v is the carrier velocity. In a “thin” device [17], where $w\sim1$ μm this corresponds to $\sim$16nA so that the current can be expected to grow in its exponential mode by a couple of decades or so before saturating and by perhaps four decades in a “thick” device, where $w\sim100$ μm.

Alternatively, if the ballast resistor is small then the increasing space charge associated with the avalanche current will eventually start to distort the electric field profile in the multiplication region and the current will again saturate. The current carried by N carriers of charge q in the depletion region is given by $I=Nqv/w$. If these charges are spread uniformly across the diode cross sectional area A then the resulting electric field dropped across the depletion region is given from Poisson's equation by $\Delta E=Nq/(A\varepsilon)=Iw/(A\varepsilon v)$, where ε is the electrical permeability. This field becomes comparable with the breakdown field, VB/w when $I\sim VBA\varepsilon v/w2$, where VB is the breakdown voltage, by which time the current has increased by a factor $\sim VBA\varepsilon/(qw)$ over its primary value. In a “thin” device of diameter $\sim$10 μm say, where $VB\sim10$ V the current can grow exponentially by some three orders of magnitude before it begins to saturate because of space charge effects. In fact carriers of opposite charges will partially cancel in the resulting the space charge so that the exponential current range estimated here represents a lower bound.

When an APD is operated below breakdown, in analogue multiplication mode, its frequency response is determined both by the initial transient behavior of the impulse response current, which depends on the carrier injection conditions, and also by the exponential decay, discussed here. In this case the transient behavior dominates the speed since the response at longer times is de-weighted by the exponential decay of the current. Conversely, when the device is used above breakdown in the Geiger mode the initial transient behavior is relatively insignificant. The exponential growth of the mean current impulse response then dominates the speed, since the current must grow by several orders of magnitude before a breakdown event is registered. Numerical simulations of the mean current impulse response in both modes, using a technique which allows for nonuniform carrier velocities, illustrate these arguments and show that in Geiger mode an order of magnitude estimate of the time dependence of the mean impulse response current may be obtained from the exponential growth rate, assuming that its initial value is given by the injected primary current.

Our analytical arguments show that both the pdf of the avalanche duration and the mean squared impulse response current below breakdown fall with the same exponential decay rate as the mean current, so that the current standard deviation falls at one half of this rate. By contrast, above breakdown the mean squared current increases with twice the exponential growth rate of the mean current, so that the standard deviation in current grows at the same rate as the mean.

The jitter, taken here as the standard deviation in time before the mean current reaches some predetermined value, is predicted, at long times, to fall below breakdown at an exponential rate $\gamma/2$. Above breakdown, after the initial transients have died away and the avalanche current triggered by absorption of a single photon rises to measurable values, this jitter becomes independent of time, and hence of the mean current, while this is still growing exponentially.

ACKNOWLEDGMENT

The authors wish to thank Prof V. Hutson for useful discussions on the general solution of (3) and (4).

References

1. M. M. Hayat, B. E. A. Saleh, "Statistical properties of the impulse response function of double carrier multiplication avalanche photodiodes including the effects of dead space", *J. Lightwave Technol.*, vol. 10, pp. 1415-1425, 1992.

2. K. B. Athreya, P. E. Ney, Branching Processes, Germany, Berlin:Springer-Verlag, 1972.

3. P. J. Hambleton, S. A. Plimmer, J. P. R. David, G. J. Rees, "Simulated current response in avalanche photodiodes", *J. Appl Phys.*, vol. 91, pp. 2107-2111, 2002.

4. P. J. Hambleton, S. A. Plimmer, G. J. Rees, "Limitations of the saturated drift velocity approximation for time domain modeling", *Semicond. Sci. Technol.*, vol. 17, pp. 124-128, 2002.

5. P. J. Hambleton, B. K. Ng, S. A. Plimmer, J. P. R. David, G. J. Rees, "The effects of nonlocal impact ionization on the speed of avalanche photodiodes", *IEEE Trans. Electron Devices*, vol. 50, no. 3, pp. 347-351, Mar. 2003.

6. D. S. Ong, J. P. R. David, G. J. Rees, "Avalanche speed in thin avalanche photodiodes", *J. Appl. Phys.*, vol. 93, pp. 4232-4239, 2003.

7. J. S. Ng, C. H. Tan, B. K. NG, P. J. Hambleton, J. P. R. David, G. J. Rees, A. H. You, D. S. Ong, "Effect of dead space on avalanche speed", *IEEE Trans. Electron Devices*, vol. 49, no. May, pp. 544-549, 2002.

8. C. H. Tan, P. J. Hambleton, J. P. R. David, R. C. Tozer, G. J. Rees, "Calculation of APD impulse response using a space- and time-dependent ionization probability distribution function", *J. Lightwave Technol.*, vol. 21, pp. 155-159, 2003.

9. M. M. Hayat, G. Dong, "A new approach for computing the bandwidth statistics of avalanche photodiodes", *IEEE Trans. Electron Devices*, vol. 47, no. 11, pp. 1273-1279, Nov. 2000.

10. J. S. Ng, C. H. Tan, J. P. R. David, G. J. Rees, "A general method for estimating the duration of avalanche multiplication", *Semicond. Sci. Technol.*, vol. 17, pp. 1067-1071, 2002.
11. B. Jacob, P. N. Robson, J. P. R. David, G. J. Rees, "Fokker-Planck approach to impact ionization distributions in space and time", *J. Appl. Phys.*, vol. 91, pp. 5438-5441, 2002.
12. S. A. Plimmer, J. P. R. David, B. Jacob, G. J. Rees, "Impact ionization probabilities as functions of two dimensional space and time", *J. Appl. Phys.*, vol. 89, pp. 2742-2751, 2001.
13. P. J. Hambleton, S. A. Plimmer, J. P. R. David, G. J. Rees, "Time response modeling in submicron avalanche photodiodes", *Int. Elect. Engineering Proc. Optoelectronics*, vol. 150, pp. 167-170, 2003.
14. P. J. Hambleton, J. P. R. David, G. J. Rees, "Enhanced carrier velocity to early impact ionization", *J. Appl. Phys.*, 2005.
15. R. J. McIntyre, "A new look at impact ionization-Part I: A theory of gain noise breakdown probability and frequency response", *IEEE Trans. Electron Devices*, vol. 46, no. 11, pp. 1623-1631, Nov. 1999.
16. A. Spinelli, A. L. Lacaita, "Physics and numerical simulation of single photon avalanche diodes", *IEEE Trans. Electron Devices*, vol. 44, no. 12, pp. 1931-1943, Dec. 1997.
17. S. Cova, M. Ghioni, A. Lacaita, C. Samori, F. Zappa, "Avalanche photodiodes and quenching circuits for single photon detection", *Appl. Opt.*, vol. 35, pp. 1956-1988, 1996.